Ultrahigh-Resolution Electro-Optic Vector Analysis for Characterization of High-Speed Electro-Optic Phase Modulators

Min Xue, *Member, IEEE*, Yuqing Heng, and Shilong Pan, *Senior Member, OSA*

***Abstract*—We propose and experimentally demonstrate an electro-optic vector analyzer (EOVA), which measures not only the magnitude but also the phase responses of high-speed electro-optic phase modulators with potentially 100-GHz measurement range and sub-Hz frequency resolution, for the first time to the best of our knowledge. The key component in the EOVA is an accurately calibrated phase modulation to intensity modulation (PM-IM) convertor, which converts the phase-modulated signal generated by the phase modulator under test into an intensity-modulated signal. After simply direct photodetection in a photodetector, the magnitude and phase information is extracted in the electrical domain. Removing the responses of the PM-IM convertor and the photodetector from the measured overall responses, the magnitude and phase responses of the phase modulator are achieved. The proposed EOVA is immune to the residual amplitude modulation in the phase modulator when an optical Hilbert transformer serves as the PM-IM convertor. In an experiment, the magnitude and phase responses of a lithium niobate high-speed phase modulator from 100 MHz to 42 GHz are precisely measured with a frequency resolution of 10 MHz.**

***Index Terms*—Electro-optic phase modulator, electro-optic vector analysis, measurement techniques, microwave photonics, optical variables measurement.**

I. Introduction

FEATURING high linearity, low insertion loss and inherent bias-free operation, electro-optic phase modulators are widely used in coherent optical communication [1], optical frequency comb generation [2], microwave photonic signal processing [3] and photonics-based microwave measurement [4] for implementing broadband electrical-to-optical conversion. The frequency responses, including the magnitude and phase responses, are the key parameters of the phase modulator, which are required to be precisely measured in the fabrication and application. Since no AC term can be directly obtained from the phase-modulated signal, the frequency responses of the phase modulator cannot be measured using a lightwave component analyzer based on electrical vector network analyzer [5], [6].

To measure the magnitude response of the phase modulator, previously, an optical spectrum analyzer (OSA) was used to monitor the optical powers of the carrier and sidebands of the phase-modulated signals produced by RF signals with different frequencies [7], [8]. Restricted by the resolution of the OSA, the measured magnitude response has a poor resolution (typical 1.25 GHz @ 1550 nm). To improve the measurement resolution, methods based on optical interferometers were proposed, in which the magnitude response is achieved by inserting the phase modulator under test in the off-center of a Sagnac interferometer or one arm of a Mach-Zehnder interferometer [9]–[12]. Although the resolution is dramatically increased, the measurement accuracy is usually poor since the optical interferometers are very sensitive to the mechanical vibrations and thermal fluctuations. Recently, a technique based on two-tone modulation and electrical spectrum analysis was reported [13], [14], which is attractive because calibration of photodetectors (PDs) is not needed.

One key problem associated with the above approaches is that they cannot be applied to measure the phase response. For many applications based on phase modulators, knowing the phase response is as important as the magnitude response. For instance, in the coherent optical communication, the distortion introduced by the uneven electro-optic conversion should be carefully compensated, which can only be completely implemented when both the high-resolution magnitude and phase responses are achieved.

In this paper, an ultrahigh-resolution electro-optic vector analyzer (EOVA), which is able to observe both of the magnitude and phase responses of phase modulators, is proposed and experimentally demonstrated, for the first time to the best of our knowledge. In the proposed EOVA, a phase-modulated signal generated from a phase modulator under test is partially converted into an intensity-modulated signal when propagating through an accurately calibrated phase modulation to intensity modulation (PM-IM) convertor. Then, the optical signal is converted into a photocurrent by photodetection, and the magnitude and phase information is extracted. Removing the frequency

Manuscript received September 10, 2017; revised December 5, 2017; accepted December 17, 2017. Date of publication December 20, 2017; date of current version February 27, 2018. This work was supported in part by the National Natural Science Foundation of China under Grants 61705103, 61527820, and 61422108, in part by the National Key R&D Program of China (2017YFF0106900), in part by the Jiangsu Provincial Program for High-level Talents in Six Areas (DZXX-034), and in part by the "333 Project" of Jiangsu Province (BRA2015343). *(Corresponding author: Shilong Pan.)*

The authors are with the Key Laboratory of Radar Imaging and Microwave Photonics, Ministry of Education, Nanjing University of Aeronautics and Astronautics, Nanjing 211106, China (e-mail: xuemin@nuaa.edu.cn; 15651667267@163.com; pans@ieee.org).

Color versions of one or more of the figures in this paper are available online at http://ieeexplore.ieee.org.

Digital Object Identifier 10.1109/JLT.2017.2785408

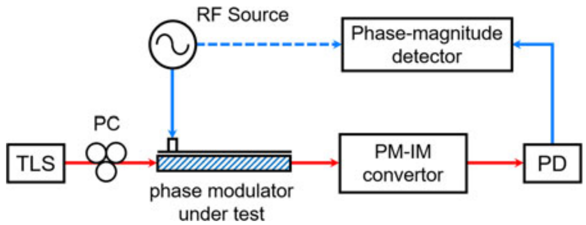

Fig. 1. Schematic diagram of the proposed EOVA. TLS, tunable laser source; PC, polarization controller; PM-IM convertor, phase modulation to intensity modulation convertor; PD, photodetector.

responses of the PM-IM convertor and the PD (which are easily obtained using well-developed technology [6]), the frequency responses of the phase modulator under test are acquired. Benefiting from the ultra-high resolution frequency sweeping and the mature magnitude and phase extraction in the electrical domain, the proposed EOVA can potentially characterize the phase modulator with a resolution as high as sub-Hz. In addition, when the PM-IM convertor is implemented by an optical Hilbert transformer, the EOVA is immune to the residual amplitude modulation of phase modulators. In an experiment, the magnitude and phase responses of a lithium niobate phase modulator from 100 MHz to 42 GHz were measured with a resolution of 10 MHz.

II. Analytical Analysis

Fig. 1 shows the schematic diagram of the proposed EOVA to measure the magnitude and phase responses of a high-speed electro-optic phase modulator. An optical carrier with an angular frequency of ω_c from a tunable laser source (TLS) is sent to a phase modulator under test, in which the optical carrier is modulated by a RF signal with a frequency of ω_e from a RF source. A phase-modulated signal is thus generated, which can be expressed by

$$\begin{aligned} E_{\mathrm{PM}}(t) &= E_0 \exp\left[i\omega_c t + i\beta \sin(\omega_e t)\right] \\ &= E_0 \exp(i\omega_c t) \sum_{-\infty}^{+\infty} J_m(\beta) \exp(im\omega_e t) \end{aligned} \quad (1)$$

where E_0 is the amplitude of the optical carrier, $J_n(\bullet)$ is the nth-order Bessel function of the first kind and β is the modulation index.

In small signal modulation case, we can only consider the optical carrier and two first-order sidebands, so the phase-modulated signal in the frequency domain can be simplified to

$$\begin{aligned} &E_{\mathrm{PM}}(\omega) = -E_0 J_1(\beta)\,\delta\left[\omega - (\omega_c - \omega_e)\right] \\ &+ E_0 J_0(\beta)\,\delta(\omega - \omega_c) + E_0 J_1(\beta)\,\delta\left[\omega - (\omega_c + \omega_e)\right] \end{aligned} \quad (2)$$

When the optical signal goes through a PM-IM convertor, the magnitude and the phase of the optical carrier and the sidebands are changed. The electric field of the propagated optical signal can be written as

$$\begin{aligned} E_m(\omega) &= E_{\mathrm{PM}}(\omega) \cdot H_c(\omega) \\ &= -E_0 J_1(\beta) H_c(\omega_c - \omega_e)\,\delta\left[\omega - (\omega_c - \omega_e)\right] \\ &\quad + E_0 J_0(\beta) H_c(\omega_c)\,\delta(\omega - \omega_c) \\ &\quad + E_0 J_1(\beta) H_c(\omega_c + \omega_e)\,\delta\left[\omega - (\omega_c + \omega_e)\right] \end{aligned} \quad (3)$$

where $H_c(\omega)$ is the transmission function of the PM-IM convertor, which can be precisely measured by an ultrahigh-resolution optical vector analyzer (OVA) based on optical single-sideband (OSSB) modulation [15]. Then, by photodetection, the optical signal is converted into a photocurrent, with its AC term given by

$$\begin{aligned} i(\omega_e) = \eta E_0^2 J_0(\beta) J_1(\beta) &\left[H_c(\omega_c + \omega_e) H_c^*(\omega_c)\right. \\ &\left. - H_c(\omega_c) H_c^*(\omega_c - \omega_e)\right] \end{aligned} \quad (4)$$

where η is the responsivity of PD. According to (4), the frequency responses of the phase modulator under test can be obtained, which is

$$H(\omega_e) = J_0(\beta) J_1(\beta) = \frac{i(\omega_e)}{\eta E_0^2 \alpha(\omega_e)} \quad (5)$$

where $\alpha(\omega)$ is a factor related to the transmission function of the PM-IM convertor, which can be expressed as

$$\alpha(\omega_e) = H_c(\omega_c + \omega_e) H_c^*(\omega_c) - H_c(\omega_c) H_c^*(\omega_c - \omega_e) \quad (6)$$

As can be seem from (5), to achieve the PM-IM conversion, it should make sure that $\alpha(\omega) \neq 0$, which requires the optical device having different frequency responses on the two sides of the optical carrier. Optical filters (having different magnitude responses on the two sidebands) and optical Hilbert transformers (having different phase responses on the two sidebands) can therefore serve as the PM-IM convertor. Moreover, the dynamic range of the measurement system is related to $\alpha(\omega)$. Larger $\alpha(\omega)$ leads to higher photocurrents from the calibrated photodetector, and accordingly larger range power detection and more accurate magnitude and phase extraction. If $\alpha(\omega)$ is increased, the dynamic range and the measurement accuracy could be boosted.

III. Experimental Results

An experiment based on the setup shown in Fig. 1 is carried out. An optical carrier with a wavelength of 1550.018 nm is generated from a tunable laser source (TLS, Agilent N7714A), which is modulated by a RF signal from an electrical vector network analyzer (VNA, R&S ZVA67) at a lithium niobate phase modulator under test. The phase modulator is manufactured by EOSPACE Inc, having a maximal modulation date rate of 40 Gb/s. A programmable optical filter (Finisar WaveShaper 16000 s) is employed to serve as the PM-IM convertor, which can be reconfigured by pre-designed programs to an optical Hilbert transformer or a bandpass filter. Then, a 50-GHz photodetector (U^2T XPDV2120R) is inserted to convert the optical signal into a photocurrent. The magnitude and phase of the AC term of the photocurrent are extracted by the phase-magnitude

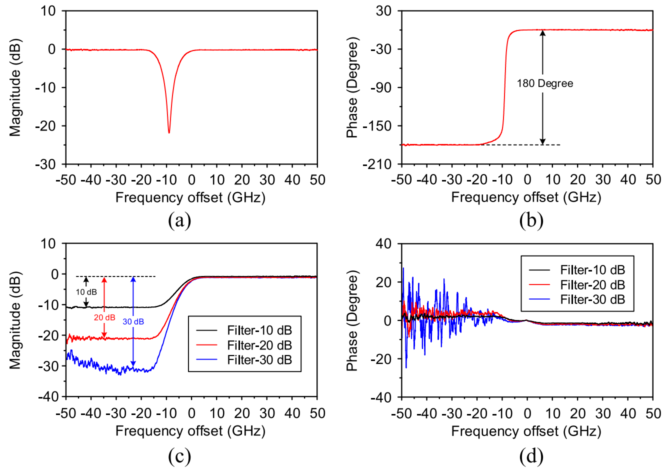

Fig. 2. The (a) magnitude and (b) phase responses of the optical Hilbert transformer; the (c) magnitude and (d) phase responses of the optical filters with different stopband attenuations.

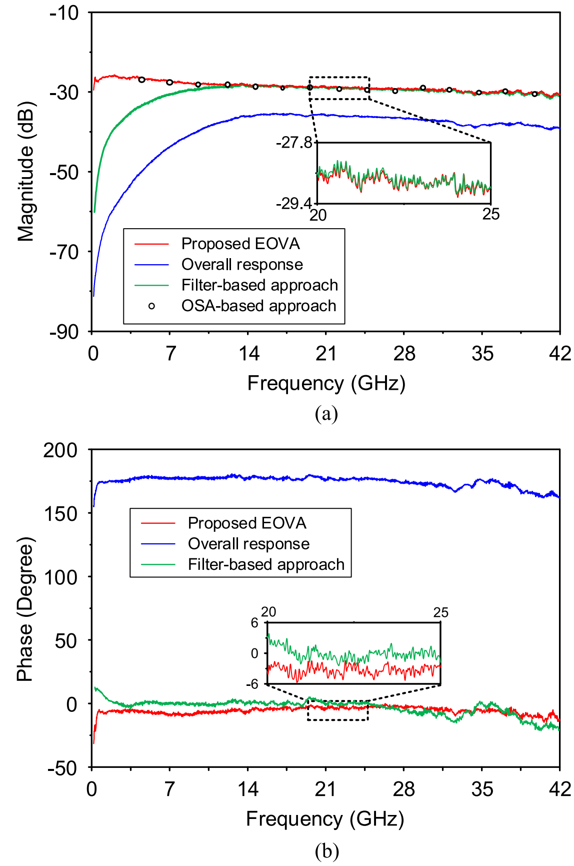

Fig. 3. The (a) magnitude and (b) phase responses of the phase modulator measured by the OSA-based approach, the filter-based approach and the proposed EOVA when an optical Hilbert transformer serves as the PM-IM convertor.

detector in the VNA. The high-resolution responses of the PM-IM convertors are measured by the OSSB-based OVA [15] and the frequency responses of the PD is achieved by a lightwave component analyzer (LCA, Keysight N4373D).

To compare the performance of different types of PM-IM convertors for characterization of high-speed electro-optic phase modulators, both the optical Hilbert transformer and the optical bandpass filter are tested in the EOVA. Fig. 2 shows the magnitude and phase responses of the optical Hilbert transformer and the optical bandpass filters with stopband attenuation of 10, 20 and 30 dB implemented by the programmable optical filter, which are measured by the OSSB-based OVA with a resolution of 10 MHz in a range of 100 GHz (from −50 to 50 GHz offset the optical carrier).

Fig. 3 shows the magnitude and phase responses of the phase modulator under test measured by the proposed EOVA when the optical Hilbert transformer serves as the PM-IM convertor. The power of the frequency-swept RF signal is set to 10 dBm, corresponding to a modulation index of 0.59 rad @ 10 GHz. In the measurement, the measurement range is 41.9 GHz (from 100 MHz to 42 GHz) and the resolution is 10 MHz. The blue line in Fig. 3 is the overall frequency responses, which contains the responses of the phase modulator, the PM-IM convertor and the photodetector. After removing the responses of the optical Hilbert transformer measured by the OSSB-based OVA and the responses of the PD measured by the LCA, the magnitude and phase response of the phase modulator is achieved (red line in Fig. 3). As a comparison, the frequency responses measured by the conventional OSA-based approach and the filter-based approach are also plotted. As can be seen, the magnitude responses measured by the proposed EOVA and the OSA-based approach are coincided. Benefiting from the high resolution of the proposed EOVA, the fine structures in the frequency responses can be clearly observed (as shown the insets in Fig. 3), which is unachievable for the conventional OSA-based approach. The magnitude response measured by the filter-based approach has good coincidence with that measured by the proposed EOVA at high frequencies, while the deviation grows rapidly with the decrease of the frequency due to the gentle roll-off of the optical bandpass filter. By the filter-based approach and the proposed EOVA, the phase responses can be achieved, as shown in Fig. 3(b). Due to the phase fluctuation in the passband of the optical filter, the phase response measured by the filter-based approach contains considerable measurement errors. It should be noted that the frequency responses measured by the proposed EOVA contain evident measurement errors at low frequencies, because the optical Hilbert transformer is unideal around the optical carrier, as shown in Fig. 2(a) and (b), which leads to the low PM-IM conversion efficiency.

According to the analytical analysis, all the optical devices having different frequency responses on the two sides of the optical carrier can serve as the PM-IM convertor for characterizing high-speed electro-optic phase modulators. Therefore, the optical Hilbert transformer and the optical bandpass filters with stopband attenuation of 10, 20 and 30 dB are respectively used as the PM-IM convertor in the experiment. The measured magnitude and phase responses of the phase modulator are shown in Fig. 4. As can be seen, when the PM-IM convertor is respectively achieved by an optical Hilbert transformer or an optical

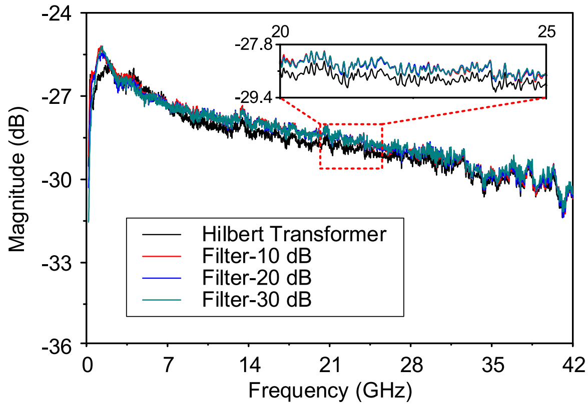

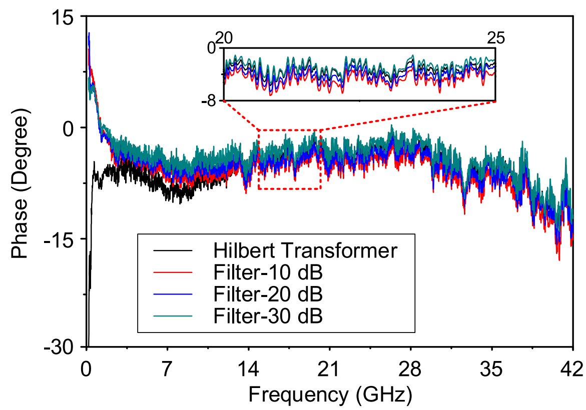

Fig. 4. The (a) magnitude and (b) phase responses measured by the proposed EOVA when an optical Hilbert transformer or an optical filter is used as the PM-IM convertor.

bandpass filter, the measured magnitude and phase responses are almost coincided. Nevertheless, small differences between the frequency responses measured in different cases can still be found, which are due to the measurement errors induced by the high-order sidebands, as will be analyzed in the following part.

IV. Measurement Error Analysis

Theoretically, only in a small modulation index case, the phase modulator under test can be accurately characterized by the proposed EOVA. To enlarge the dynamic range, the phase modulator usually works at a large modulation index. However, with the increase of the modulation index, the high-order sidebands arise and their beat notes would introduce considerable measurement errors and deteriorate the measured results. Considering the case of large modulation index, the AC term of the photocurrent can be written as

$$
\begin{aligned}
i_m\left(\omega_e\right) &= \eta E_0^2 J_0\left(\beta\right) J_1\left(\beta\right)\left[H_c\left(\omega_c+\omega_e\right) H_c^*\left(\omega_c\right)\right. \\
&\quad \left.-H_c\left(\omega_c\right) H_c^*\left(\omega_c-\omega_e\right)\right]+\eta E_0^2 \sum_{\substack{m=-\infty \\ m\neq -1,0}}^{+\infty} J_{m+1}\left(\beta\right) J_m\left(\beta\right) \\
&\quad \times H_c\left[\omega_c+\left(m+1\right)\omega_e\right] H_c^*\left(\omega_c+m\omega_e\right)
\end{aligned}
\tag{7}
$$

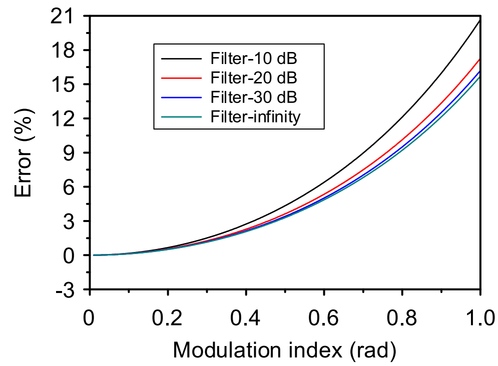

Fig. 5. The magnitude errors introduced by the high-order sidebands when the optical bandpass filters with different stopband attenuations and an ideal bandpass filter are respectively applied.

Thus, the measured frequency responses are

$$
\begin{aligned}
H_m\left(\omega_e\right) &= \frac{i_m\left(\omega_e\right)}{\eta E_0^2 \alpha\left(\omega_e\right)} \\
&= J_0\left(\beta\right) J_1\left(\beta\right) \\
&\quad + \frac{1}{\alpha\left(\omega_e\right)} \sum_{\substack{m=-\infty \\ m\neq -1,0}}^{+\infty} J_{m+1}\left(\beta\right) J_m\left(\beta\right) H_c \\
&\quad \times \left[\omega_c+\left(m+1\right)\omega_e\right] H_c^*\left(\omega_c+m\omega_e\right)
\end{aligned}
\tag{8}
$$

In (8), at the right side of the equation, the first term is the actual responses of the phase modulator, while the second term is the measurement errors introduced by the beat notes of the high-order sidebands. As can be seen, the high-order-sideband induced measurement errors are affected by not only the modulation index but also the transmission function of the optical device (i.e., $\alpha(\omega)$).

To investigate the influence of the PM-IM convertor on the measurement accuracy along with the modulation index, a numerical simulation is performed. Fig. 5 shows the magnitude errors introduced by the high-order sidebands when the optical bandpass filters with the stopband attenuation of 10, 20 and 30 dB, and an ideal bandpass filter are respectively used to achieve the PM-IM conversion. As can be seen, the error is very small in small modulation regime, which is less than 0.16% for a modulation index of 0.1. With the increase of the modulation index, the measurement errors dramatically increased. In addition, different PM-IM converters would introduce different errors. For a given modulation index, the measured responses approach the actual ones with the increase of the stopband attenuation, because the high-order-sideband induced errors are mainly determined by $1/\alpha(\omega)$ and decrease with the growth of the stopband attenuation. Even when an ideal optical bandpass filter is applied (i.e., $1/\alpha(\omega) = 1$), the measurement errors still exist as the high-order sidebands in the passband of the optical filter are remained. The high-order sidebands have no influence on the measurement of the phase response, as the ideal PM-IM convertors are used in the simulation. It should be noted that the phase responses of the PM-IM converters have no influence on

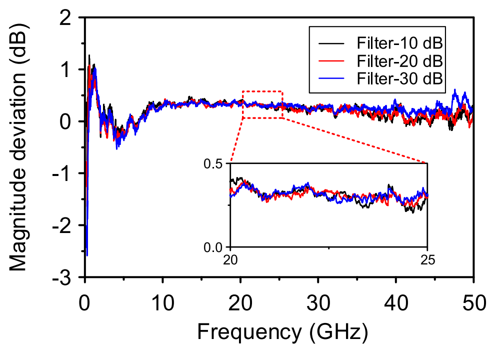

(a)

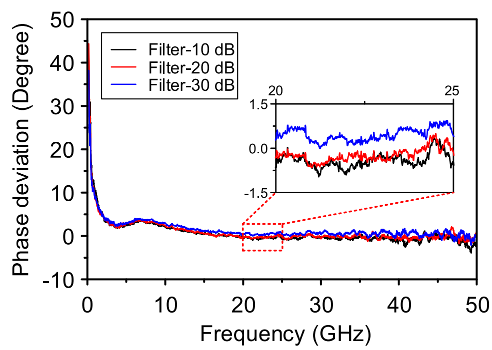

(b)

Fig. 6. The (a) magnitude and (b) phase responses measured by the optical bandpass filters deviated from those measured using the optical Hilbert transformer. The modulation index of the phase modulator is 0.59.

the high-order-sideband induced error in the simulation, as the high-order sidebands undergo the same phase change and the phase change induced by the PM-IM converter is eliminated in photodetection.

Additionally, when an optical Hilbert transformer serves as the PM-IM convertor, the measured frequency responses are not affected by the high-order sidebands since the measurement errors introduced by the negative and positive high-order sidebands have the same powers but out of phase. The measurement error induced by the residual amplitude modulation can be avoided, because the residual amplitude-modulated signal is converted into a phase-modulated signal when achieving the PM-IM conversion by the optical Hilbert transformer.

The analysis above shows that the responses can be precisely measured when an ideal Hilbert transformer is adopted to achieve the PM-IM conversion. Thereby, the responses measured by applying the optical bandpass filters with different stopband attenuations deviated from those measured by the optical Hilbert transformer are given, as shown in Fig. 6. As can be seen from Fig. 6(a), evident distortions appear at low frequencies, since the unideal optical Hilbert transformer and optical bandpass filters achieved by a programmable optical filter has low PM-IM conversion efficiency at low frequencies. The deviations at the high frequencies are introduced by the high-order sidebands, which is around 0.5 dB. The numerical simulation indicates that the high-order-sideband induced measurement errors decrease from 0.52 to 0.40 dB, when the stopband attenuation of the optical bandpass filter is increased from 10 dB towards infinity. The experimental results agree well with the simulation results.

V. Conclusion and Discussion

In conclusion, an EOVA to accurately characterize high-speed phase modulators is proposed. In the experiment, the magnitude and phase responses of a lithium niobate phase modulator from 0.1 to 42 GHz are obtained with a resolution of 10 MHz. Benefitting from the large dynamic range of the electrical VNA (typically ∼130 dB), the EOVA constructed in the experiment has a dynamic range of over 100 dB, with the degradation mainly from the insertion loss and conversion loss of the devices in the system. The frequency resolution is determined by the linewidth of the TLS, which is less than 100 kHz. By employing an ultra-narrow-linewidth laser [16], the frequency resolution can be further improved and a sub-Hz resolution could be potentially achievable. The measurement errors of the magnitude and phase are approximately 0.2 dB and 2 degree, respectively, restricted by the accuracy of the VNA and stability of the measurement system. Hundred-GHz measurement range can be achieved by employing the VNA and the PD having a working frequency range of hundreds of GHz, which is available in the market. In addition, by using an optical Hilbert transformer as the PM-IM converter, accurate measurement and large dynamic range can be simultaneously achieved.

References

[1] W. Shieh, H. Bao, and Y. Tang, "Coherent optical OFDM: theory and design," *Opt. Express*, vol. 16, no. 2, pp. 841–859, 2008.

[2] C. Chen, C. He, D. Zhu, R. Guo, F. Zhang, and S. Pan, "Generation of a flat optical frequency comb based on a cascaded polarization modulator and phase modulator," *Opt. Lett.*, vol. 38, no. 16, pp. 3137–3139, 2013.

[3] J. Yao, "Microwave photonics," *J. Lightw. Technol.*, vol. 27, no. 3, pp. 314–335, Feb. 2009.

[4] X. Zhang, H. Chi, X. Zhang, S. Zheng, X. Jin, and J. Yao, "Instantaneous microwave frequency measurement using an optical phase modulator," *IEEE Microw. Wireless Compon. Lett.*, vol. 19, no. 6, pp. 422–424, Junt. 2009.

[5] P. D. Hale and D. F. Williams, "Calibrated measurement of optoelectronic frequency response," *IEEE Trans. Microw. Theory Techn.*, vol. 51, no. 4, pp. 1422–1429, Apr. 2003.

[6] "High-speed lightwave component analysis," *Agilent Technol.*, Palo Alto, CA, USA, Application Note 1550-6, Jun. 2000.

[7] R. Tench, J.-M. Delavaux, L. Tzeng, R. Smith, L. Buhl, and R. Alferness, "Performance evaluation of waveguide phase modulators for coherent systems at 1.3 and 1.5 μm," *J. Lightw. Technol.*, vol. LT-5, no. 4, pp. 492–501, Apr. 1987.

[8] Y. Shi, L. Yan, and A. E. Willner, "High-speed electrooptic modulator characterization using optical spectrum analysis," *J. Lightw. Technol.*, vol. 21, no. 10, pp. 2358–2367, Oct. 2003.

[9] E. H. Chan and R. A. Minasian, "A new optical phase modulator dynamic response measurement technique," *J. Lightw. Technol.*, vol. 26, no. 16, pp. 2882–2888, Aug. 2008.

[10] F. P. Romstad, D. Birkedal, J. Mork, and J. Hvam, "Heterodyne technique for measuring the amplitude and phase transfer functions of an optical modulator," *IEEE Photon. Technol. Lett.*, vol. 14, no. 5, pp. 621–623, 2002.

[11] J. A. Campbell, A. Knoesen, and D. R. Yankelevich, "Measurement of the modulation efficiency of an optical phase modulator using a self-homodyne receiver," *IEEE Photon. Technol. Lett.*, vol. 14, no. 9, pp. 1330–1332, Sep. 2002.

[12] N. Caponio, P. Gambini, and M. Puleo, "Characterization of the dynamic response of a waveguide phase modulator by means of an optical frequency discriminator," *NIST Special Publ.*, vol. 792, pp. 79–82, 1990.

[13] S. Zhang, H. Wang, X. Zou, Y. Zhang, R. Lu, and Y. Liu, “Self-calibrating measurement of high-speed electro-optic phase modulators based on two-tone modulation,” *Opt. Lett.*, vol. 39, no. 12, pp. 3504–3507, 2014.

[14] S. Zhang, C. Zhang, H. Wang, X. Zou, Y. Liu, and J. E. Bowers, “Calibration-free measurement of high-speed Mach–Zehnder modulator based on low-frequency detection,” *Opt. Lett.*, vol. 41, no. 3, pp. 460–463, 2016.

[15] S. Pan and M. Xue, “Ultrahigh-resolution optical vector analysis based on optical single-sideband modulation,” *J. Lightw. Technol.*, vol. 35, no. 4, pp. 836–845, Feb. 2017.

[16] T. Kessler *et al.*, “A sub-40-mHz-linewidth laser based on a silicon single-crystal optical cavity,” *Nature Photon.*, vol. 6, no. 10, pp. 687–692, 2012.

Min Xue was born in Changzhou, China, in September 1988. He received the B.S. and Ph.D. degrees from the College of Electronic and Information Engineering, Nanjing University of Aeronautics and Astronautics, Nanjing, China, in 2011 and 2016, respectively. He joined the College of Electronic and Information Engineering, Nanjing University of Aeronautics and Astronautics, in 2016. He is currently a member of the Key Laboratory of Radar Imaging and Microwave Photonics, Nanjing University of Aeronautics and Astronautics, Ministry of Education. His research interests include photonic microwave measurement and metrology, optical fiber sensor, and integrated microwave photonics.

Yuqing Heng received the B.S. degree in electronics engineering from the Nanjing University of Aeronautics and Astronautics, Nanjing, China, in 2016. She is currently working toward the M.S. degree at the Key Laboratory of Radar Imaging and Microwave Photonics, Nanjing University of Aeronautics and Astronautics, Ministry of Education. Her research interests include photonic microwave measurement and electro-optic and optic-electro devices measurement.

Shilong Pan (S’06–M’09–SM’13) received the B.S. and Ph.D. degrees in electronics engineering from Tsinghua University, Beijing, China, in 2004 and 2008, respectively. From 2008 to 2010, he was a “Vision 2010” Postdoctoral Research Fellow with the Microwave Photonics Research Laboratory, University of Ottawa, Ottawa, ON, Canada. In 2010, he joined the College of Electronic and Information Engineering, Nanjing University of Aeronautics and Astronautics, Nanjing, China, where he is currently a Full Professor and an Executive Director of the Key Laboratory of Radar Imaging and Microwave Photonics, the Ministry of Education. His research has focused on microwave photonics, which includes optical generation and processing of microwave signals, analog photonic links, photonic microwave measurement, and integrated microwave photonics. He has authored or coauthored more than 320 research papers, including more than 170 papers in peer-reviewed journals and 150 papers in conference proceedings.

He is currently a Topical Editor for the *Chinese Optics Letters*. He was the recipient of an OSA Outstanding Reviewer Award in 2015 and a Top Reviewer for the *Journal of Lightwave Technology* in 2016. He is a Chair of numerous international conferences and workshops, including the TPC Chair of the International Conference on Optical Communications and Networks in 2015, the TPC Co-Chair for the IEEE International Topical Meeting on Microwave Photonics in 2017, the TPC Chair of the high-speed and broadband wireless technologies subcommittee of the IEEE Radio Wireless Symposium in 2013, 2014, and 2016, the TPC Chair of the Optical fiber sensors and microwave photonics subcommittee of the OptoElectronics and Communication Conference in 2015, and a Chair of the microwave photonics for broadband measurement workshop of International Microwave Symposium in 2015.